IOP Conf. Series: Materials Science and Engineering **257** (2017) 012022 doi:10.1088/1757-899X/257/1/012022

Effect of pin tool design on the material flow of dissimilar AA7075-AA6061 friction stir welds

Mohammed M Hasan[1,2*], M Ishak[1] and M R M Rejab[1]

[1]Faculty of Mechanical Engineering, Universiti Malaysia Pahang, Pahang, Malaysia
[2]University of Technology, Baghdad, Iraq

[*]Corresponding author: modmhasan@gmail.com

Abstract. Tool design is the most influential aspect in the friction stir welding (FSW) technology. Influence of pin tool geometry on material flow pattern are studied in this work during the FSW of dissimilar AA7075 and AA6061 aluminium alloys. Three truncated pin tool profiles (threaded, threaded with single flat, and unthreaded with single flat) were used to prepare the weldments. The workpieces were joined using a custom-made clamping system under 1100 rpm of spindle speed, 300 mm/min of traverse rate and 3° of tilt angle. The metallographic analysis showed that defect-free welds can be produced using the three pin tools with significant changes in the mixing stir zone structure. The results declared that the introducing of the flat on the cone of the probe deviates the pattern of the onion rings without changing the chemical composition of the created layers. This in turn improves the hardness distribution and tensile strength of the welded joint. It was also noted that both heat affected zone (HAZ) and thermal-mechanical affected zone (TMAZ) are similar in composition to their corresponding base materials (BM).

1. Introduction

Friction stir welding has become one of the widely-used technologies in modern industries, such as automotive and aerospace [1, 2]. This novel green welding method was invented in 1991 by The Welding Institute (TWI) of the UK to solve the problem of joining the hard-to-weld aluminium alloys [3, 4]. It also offered the ability of welding dissimilar materials from the same or different families, such as aluminium alloy to another aluminium alloy, aluminium to magnesium and aluminium to steel [5, 6]. This advantage permits to take the benefits of both adjoined materials [7, 8]. As seen in Figure 1, the materials to be weld are connected through this solid-state method by stirring a specially designed rotating tool, which is the main source of the process heat that not exceeds the melting point of the workpieces [9].

The success of the material mixing is mainly depending on the geometry of the tool pin or probe [10, 11] and the welding rotation speed (ω) and tool traverse rate (υ) [12]. Improper design of the pin tool may result in an internal defects or incomplete material mixing within the stir zone (SZ). For defect-free weld, the characterization of the probe design determines the flow pattern, which has not been widely considered in the previous research studies as the mechanical properties of the welding joints. Accordingly, the inspection of material flow in conjunction with tool design during the friction stir processing is vital for putting on the right track of the weld quality.

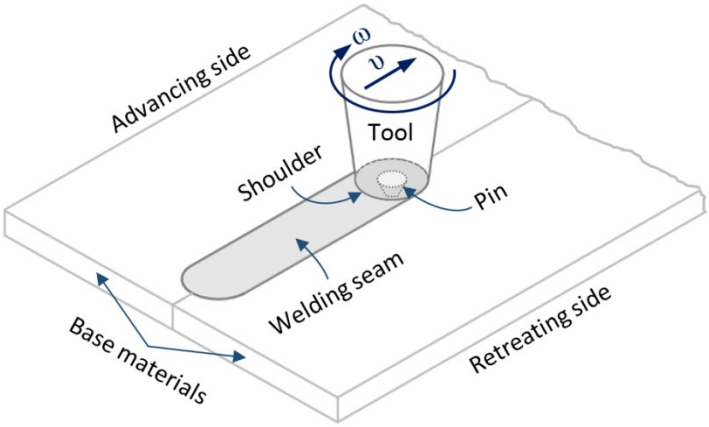

Figure 1. Schematic drawing of the FSW process.

Recently, Tongne et al. [13] studied the formation and evolution of banded structures observed in similar weld of AA6082-T6 aluminium alloy using trigonal tool. It was demonstrated that the formation of the banded structures is mainly related to the geometry of the pin whereas the friction conditions have a much smaller effect. Patel et al. [14] investigated the influence of polygonal pin profiles on friction stir processed super plasticity of AA7075-T651 aluminium alloy. They noticed that all polygonal pin profiles indicated sticking of the workpiece material around tool pin and resulted in non-uniform microstructure in the SZ. On the other hand, uniform microstructure without cavitation in the SZ was observed in the sample produced by the square pin tool. Schneider and his co-authors [15] examined the material flow modification in the FSW of AA2219-T87 aluminium alloy through introduction of flats into the threaded cylindrical pin tools. Significant changes in the FSW structure with varying numbers of flats were observed, but without significant changes in tensile strength. Changes in the textural banding shape, the addition of sub-bands, and a new set of bands from coalescence of band kinks constitute the structural changes observed. Based on the material flow characteristics, a mechanism of the friction stir AA7020-T6 weld formation was presented by Kumar and Kailas [16]. They stated that there are two different modes of material flow regimes involved in the friction stir weld formation; namely “pin-driven flow” and “shoulder-driven flow”. These material flow regimes merge together to form a defect-free weld. It was also illustrated that the etching contrast in these regimes gives rise to the onion ring pattern in friction stir welds. Formation mechanism of these onion rings was rather difficult to be explained. Krishnan [17] attributed the creation of the onion rings to the process of friction heating due to the tool rotation and forward movement, which extrudes the metal around to the retreating side of the tool.

In the FSW of dissimilar alloys or materials, limited articles focused on the material flow and mixing, especially with the effect of tool design. Consequently, this paper aims to investigate the influence of the pin tool profile on the microstructure of the dissimilar AA7075-AA6061 friction stir welds. This study contributes to the advanced industrial technology.

2. Experimental set up

Welding coupons were prepared from 3-mm-thick AA7075-T6 and AA6061-T6 aluminium alloys, whose mechanical properties are presented in Table 1. The specimens were cut and ground by a precision grinding machine to the final dimensions of 125×50 mm and cleaned with acetone. According to our previous work [18], a specially designed clamping system was used to produce the welds, as shown in Figure 2. Butt-joints were formed in a route parallel to the rolling direction of the base materials.

Table 1. Mechanical properties of the base materials (normal to the rolling direction).

Alloy	Yield strength (MPa)	Tensile strength (MPa)	Vickers hardness	Elongation (%)
AA7075-T6	503	571	175	11
AA6061-T6	276	307	107	12

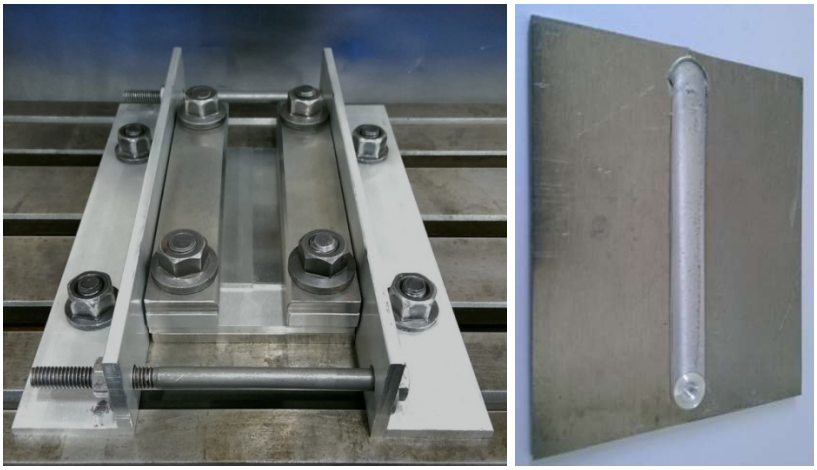

Figure 2. The custom-made clamping system and a sample photograph of the welding joint.

Three different welding pin tools, whose geometry are schematically viewed in Figure 3, were fabricated from H13 steel. Each tool consisted of concave shoulder of 12-mm-diameter and 8° of concave angle. The base diameter of the probes was 4 mm, which truncated through 10° along the length of 2.7 mm. The cone of the probe was threaded with M4×1 left-hand threads in the first and second tools, while it left smooth in the third one. A single flat was formed in the second and third tapered pin tools. Based on the results of our previous research studies [19, 20], the softer AA6061 alloy was placed on the advancing side (AS) of the weld and the tool rotation speed, traverse rate and tilt angle were fixed at 1100 rpm, 300 mm/min and 3°, respectively.

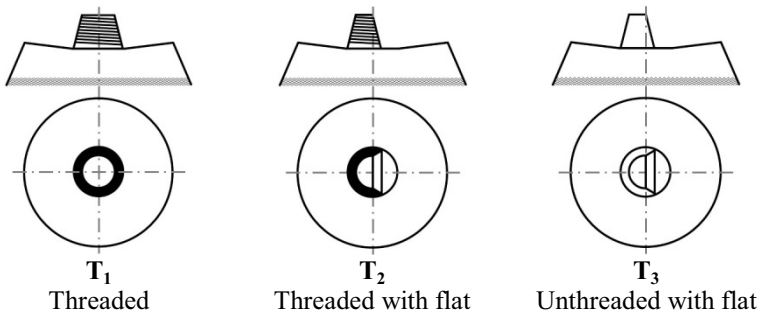

Figure 3. Schematic views of the three welding pin tools.

The produced welds were left two months for natural aging [21]. After that, tensile and metallographic specimens were cut by a wire cutting machine. The specimens were prepared as per the standard of American Society for Testing of Materials (ASTM: E8-11). Tests were then conducted at room temperature using a 50 kN universal testing machine with a speed of 1 mm/min. Three tension tests were conducted for each case study, and the average ultimate tensile strength and elongation were considered. The standard guide for preparation of metallographic specimens (ASTM: E3-11) was followed to prepare the metallographic specimens, which were then etched by a modified killer's

reagent to reveal the grain structure of the weld zone. Hardness distribution were then observed across the weld centreline, in a direction normal to the weld seam, by a Vickers micro-hardness tester using HV0.5 test method with an indent time of 10 seconds. The metallographic analysis was performed using an optical microscope and scanning electron microscope (SEM) equipped with an energy dispersive spectrometry (EDS).

3. Results and discussion

The obtained micrographs showed that defect-free joints were produced using the three tools. The weld in the stir zone has exhibited the well-recognized onion rings, as seen in Figure 4. The nugget zone resulted from the threaded tools T_1 (without flat) and T_2 (with single flat) were compared to the that produced by T_3, which consisted of a non-threaded probe with additional flat.

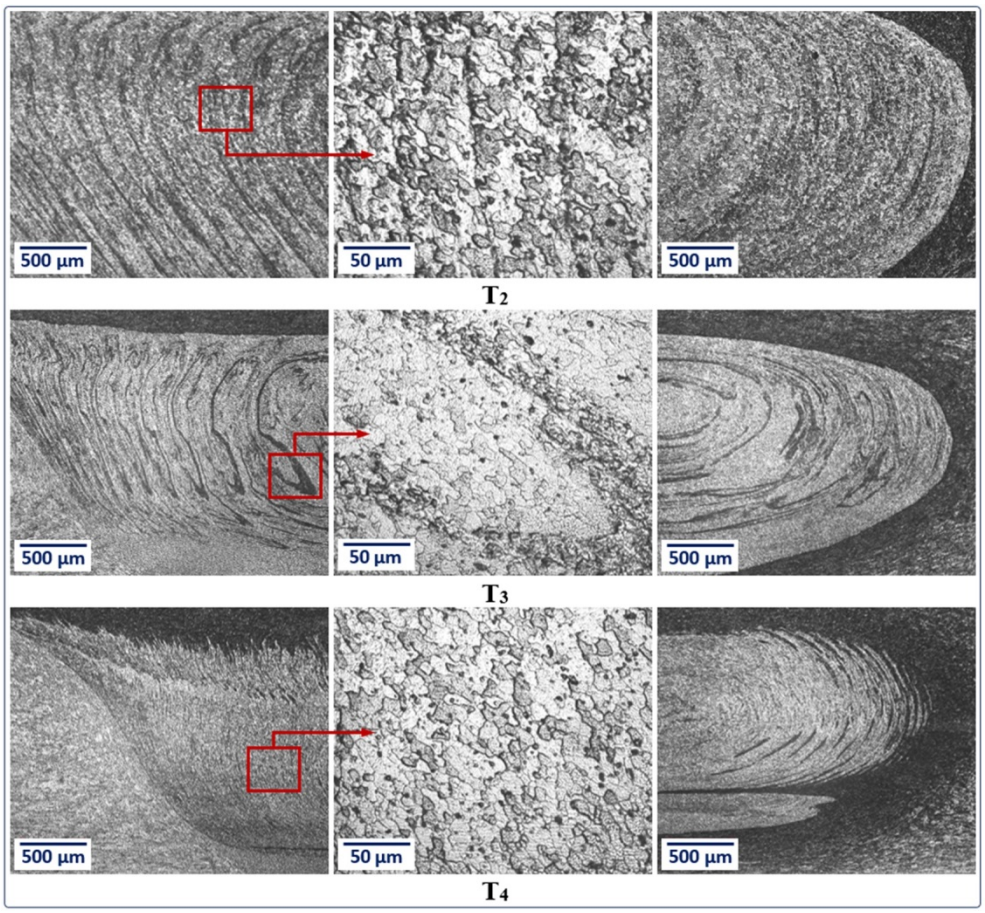

Figure 4. Microstructure of the welding stir zone related to the pin tool design.

The onion rings appeared more uniform when the threaded pin tool T_1 was used, while they nearly vanished when the unthreaded tool T_3 was used. This is due to that when using a threaded probe in similar and dissimilar FSW, the material moves downward and a helical vertical rotational flow within the intermixed region generates beside the periphery of the rotating pin and hence forming the sub-layers or onion rings [22]. The shape of the rings was significantly changed when a flat was added to the cone of the threaded pin tool T_2. The flat pushed the abutting materials away from the probe and reduced the effect of the threads.

Chemical composition of the weld was analysed in the onion rings, TMAZ, HAZ, and BM. The etching response of the dissimilar parent materials to the Keller's reagent are not the same due to the difference in their chemical composition [23]. For this reason, the micrographs revealed in dark and

bright colours, as shown in Figure 5, which represents the SEM image of the onion rings and the corresponding EDS spectrum.

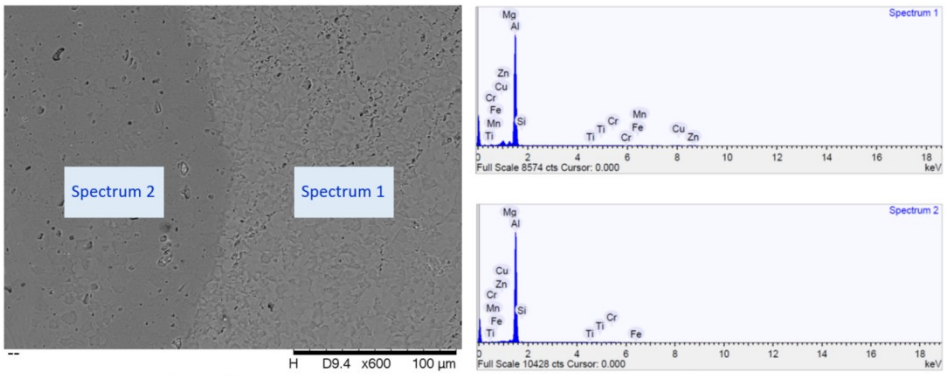

Figure 5. The SEM image of the onion ring layers and the corresponding EDS spectrums.

The results presented in Table 2 clarify that the bright region is similar in composition to that of the AA7075-T6 base alloy, while the dark one is identical in composition to the softer AA6061-T6 base material. Same observation was found in the works of İpekoğlu and Çam [24] and Guo et al. [25]. On the other hand, the composition of the TMAZ and HAZ of both welding sides are close to their corresponding base materials.

Table 2. The acquired chemical composition (wt.%) of the base materials, HAZ, TMAZ and the onion ring layers related to the spectrums shown in Figure 5.

Spectrum	Si	Fe	Cu	Mn	Mg	Cr	Zn	Ti	Al
1	0.543	0.183	2.261	0.031	2.610	0.224	5.203	0.136	Balance
2	0.720	0.322	1.046	0.018	1.077	0.090	0.393	0.072	Balance
TMAZ-6061	0.716	0.046	0.185	0.040	1.036	0.320	0.227	0.039	Balance
TMAZ-7075	0.097	0.241	1.943	0.061	2.704	0.196	5.853	0.115	Balance
HAZ-6061	0.716	0.046	0.185	0.040	1.036	0.320	0.227	0.039	Balance
HAZ-7075	0.097	0.241	1.943	0.061	2.704	0.196	5.853	0.115	Balance
BM-6061	0.701	0.090	0.161	0.023	0.801	0.258	0.215	0.047	Balance
BM-7075	0.168	0.212	1.801	0.040	2.512	0.251	5.525	0.132	Balance

As shown in Figure 6, the joint strength was not highly affected by the creation of the different layers or onion rings. The ultimate tensile strength of the weld ranged from 229.5 MPa for tool T_3, passing through 237.6 MPa for T_1 to reach the maximum value of 252.1 MPa for T_2. Since the joint strength of dissimilar friction stir weld is typically compared to the softer material [26], tensile strength of the harder AA7075 base material was not shown in the graph. These outcomes are coincide with the observation of Schneider and his research group [27]. They found that the existence of flat/flute in the pin tool design changes the flow pattern of the mixed materials without significant change in the weld strength. Figure 7 presents the micro-hardness distribution along the transvers centreline of the weld related to the welding pin tools. Overall, the welding joints have exhibited a noticeable decrease in the level of the Vickers hardness number (VHN) compared to the base materials. This could be attributed to the grain refinement or recrystallization within the stir zone and the over-aging in the heat affected zone [2, 28, 29].

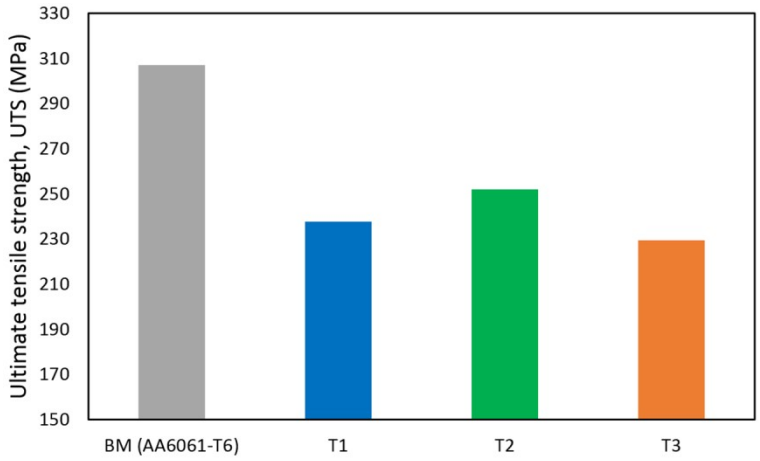

Figure 6. Tensile strength of the weld related to pin tool design.

Maximum reduction of the weld hardness was observed in the HAZ of the AA6061-T6 alloy, which was fixed on the AS. The lowest hardness values of 66, 71 and 63 were measured in the welding joints produced by the welding tools T_1, T_2 and T_3, respectively. The fracture of the tension test specimens was initiated from the corresponding locations of these minimum hardness values at the HAZ. It has been reported that the fracture takes place in the weakest region during the tension test of the similar and dissimilar friction stir welds of aluminium alloys. In case of defect-free dissimilar friction stir welds, the HAZ of the softer alloy represents the weakest region, where the fracture commonly occurs [24, 30]. It is obvious that the results of tension tests are proportional with the hardness level at the HAZ of the softer material. In other word, the minimum joint strength was measured in the specimen that exhibited the lowest VHN and vice versa.

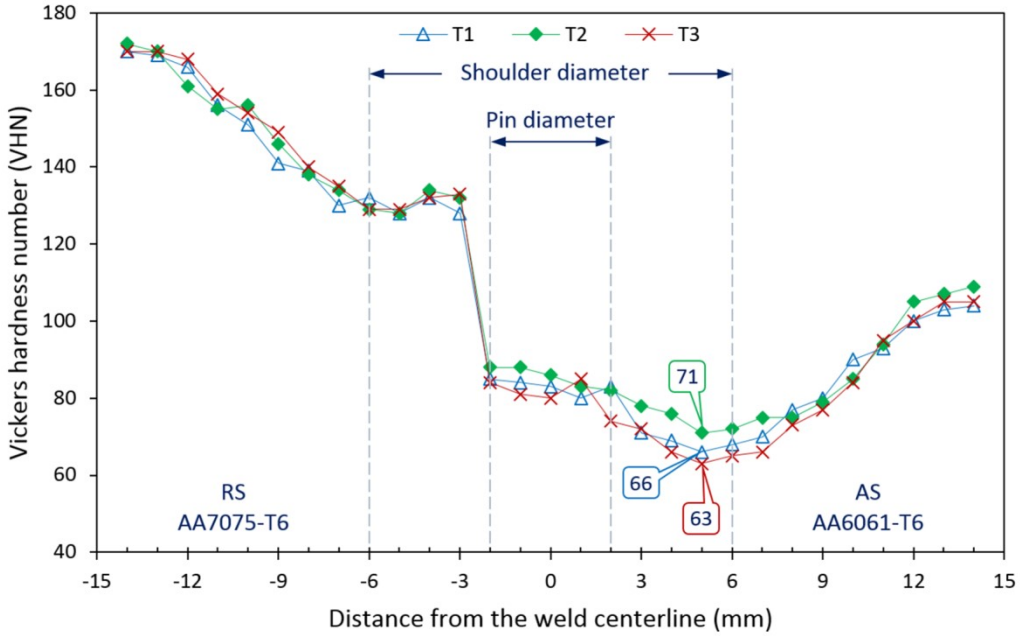

Figure 7. Hardness distribution of the weld related to the pin tool design.

4. Conclusions

The outcomes of this research showed that there is a clear relation between the design of the welding pin tool and the material flow pattern of dissimilar friction stir welds. Formation of the well-known onion rings is found to be sensitive to the profile of the probe. The introducing of a flat on the cone of

the pin tool changes the flow pattern within the mixing stir zone and affect the hardness distribution, and hence the tensile strength of the welding joint. The etching response showed different layers in dark and bright colours inside the weld nugget, which are similar to their corresponding base materials. The chemical compositions of the TMAZ and HAZ regions were not change during the FSW process.

Acknowledgements
The authors would like to be obliged to the Malaysian Ministry of Education for providing research grant (RDU1403114). Thanks to Universiti Malaysia Pahang for laboratory facilities.

References

[1] Sathari N, Razali A, Ishak M and Shah L 2015 Mechanical strength of dissimilar AA7075 and AA6061 aluminum alloys using friction stir welding *International Journal of Automotive & Mechanical Engineering* **11** 2713-21
[2] Ahmed M, Ataya S, Seleman M E-S, Ammar H and Ahmed E 2017 Friction stir welding of similar and dissimilar AA7075 and AA5083 *J. Mater. Process. Technol.* **242** 77-91
[3] Selamat N, Baghdadi A, Sajuri Z and Kokabi A 2016 Friction stir welding of similar and dissimilar aluminium alloys for automotive applications *International Journal of Automotive & Mechanical Engineering* **13**
[4] Zhou Z, Yue Y, Ji S, Li Z and Zhang L 2016 Effect of rotating speed on joint morphology and lap shear properties of stationary shoulder friction stir lap welded 6061-T6 aluminum alloy *Int. J. Adv. Manuf. Technol.* 1-7
[5] Sahu P K, Pal S, Pal S K and Jain R 2016 Influence of plate position, tool offset and tool rotational speed on mechanical properties and microstructures of dissimilar Al/Cu friction stir welding joints *J. Mater. Process. Technol.* **235** 55-67
[6] Shi H, Chen K, Liang Z, Dong F, Yu T, Dong X, Zhang L and Shan A 2016 Intermetallic Compounds in the Banded Structure and Their Effect on Mechanical Properties of Al/Mg Dissimilar Friction Stir Welding Joints *J. Mater. Sci. Technol.*
[7] Shah L H and Ishak M 2014 Review of Research Progress on Aluminum–Steel Dissimilar Welding *Mater. Manuf. Processes* **29** 928-33
[8] Islam M R, Ishak M, Shah L H, Idris S R A and Meriç C 2016 Dissimilar welding of A7075-T651 and AZ31B alloys by gas metal arc plug welding method *Int. J. Adv. Manuf. Technol.* **88** 2773-83
[9] NAA S and AR R 2014 Investigation of Single-pass Double-pass Techniques on Friction Stir Welding of Aluminium *Journal of Mechanical Engineering and Sciences (JMES)* **7** 1053-61
[10] García-Bernal M, Mishra R, Verma R and Hernández-Silva D 2016 Influence of friction stir processing tool design on microstructure and superplastic behavior of Al-Mg alloys *Mat. Sci. Eng. A-Struct.* **670** 9-16
[11] Mehta K P and Badheka V J 2017 Influence of tool pin design on properties of dissimilar copper to aluminum friction stir welding *Transactions of Nonferrous Metals Society of China* **27** 36-54
[12] Pan Y and Lados D A 2017 Friction Stir Welding in Wrought and Cast Aluminum Alloys: Weld Quality Evaluation and Effects of Processing Parameters on Microstructure and Mechanical Properties *Metallurgical and Materials Transactions a-Physical Metallurgy and Materials Science* **48a** 1708-26
[13] Tongne A, Desrayaud C, Jahazi M and Feulvarch E 2017 On material flow in Friction Stir Welded Al alloys *J. Mater. Process. Technol.* **239** 284-96
[14] Patel V V, Badheka V and Kumar A 2017 Effect of polygonal pin profiles on friction stir processed superplasticity of AA7075 alloy *J. Mater. Process. Technol.* **240** 68-76
[15] Schneider J, Brooke S and Nunes A C 2015 Material Flow Modification in a FSW Through Introduction of Flats *Metall. Mater. Trans. B* **47** 720-30
[16] Kumar K and Kailas S V 2008 The role of friction stir welding tool on material flow and weld formation *Mat. Sci. Eng. A-Struct.* **485** 367-74

[17] Krishnan K 2002 On the formation of onion rings in friction stir welds *Mat. Sci. Eng. A-Struct.* **327** 246-51
[18] Hasan M M, Ishak M and Rejab M R M 2015 A simplified design of clamping system and fixtures for friction stir welding of aluminium alloys *JMES* **9** 1628-39
[19] Hasan M M, Ishak M and Rejab M R M 2017 Effect of backing material and clamping system on the tensile strength of dissimilar AA7075-AA2024 friction stir welds *Int. J. Adv. Manuf. Technol.* 1-17
[20] Hasan M M, Ishak M and Rejab M R M 2017 Influence of machine variables and tool profile on the tensile strength of dissimilar AA7075-AA6061 friction stir welds *Int. J. Adv. Manuf. Technol.* **90** 2605-15
[21] Mishra R S and Mahoney M W 2007 *Friction stir welding and processing*: ASM International)
[22] Teimurnezhad J, Pashazadeh H and Masumi A 2016 Effect of shoulder plunge depth on the weld morphology, macrograph and microstructure of copper FSW joints *J. Manuf. Processes* **22** 254-9
[23] Firouzdor V and Kou S 2010 Formation of liquid and intermetallics in Al-to-Mg friction stir welding *Metall. Mater. Trans. A* **41** 3238-51
[24] İpekoğlu G and Çam G 2014 Effects of initial temper condition and postweld heat treatment on the properties of dissimilar friction-stir-welded joints between AA7075 and AA6061 aluminum alloys *Metall. Mater. Trans. A* **45** 3074-87
[25] Guo J F, Chen H C, Sun C N, Bi G, Sun Z and Wei J 2014 Friction stir welding of dissimilar materials between AA6061 and AA7075 Al alloys effects of process parameters *Mater. Des.* **56** 185-92
[26] Giraud L, Robe H, Claudin C, Desrayaud C, Bocher P and Feulvarch E 2016 Investigation into the dissimilar friction stir welding of AA7020-T651 and AA6060-T6 *J. Mater. Process. Technol.* **235** 220-30
[27] Schneider J, Brooke S and Nunes Jr A C 2016 Material flow modification in a FSW through introduction of flats *Metall. Mater. Trans. B* **47** 720-30
[28] Sun Y, Tsuji N and Fujii H 2016 Microstructure and mechanical properties of dissimilar friction stir welding between ultrafine grained 1050 and 6061-t6 aluminum alloys *Metals* **6** 249
[29] Khan N Z, Siddiquee A N, Khan Z A and Mukhopadhyay A K 2017 Mechanical and microstructural behavior of friction stir welded similar and dissimilar sheets of AA2219 and AA7475 aluminium alloys *J. Alloys Compd.* **695** 2902-8
[30] Rodriguez R I, Jordon J B, Allison P G, Rushing T and Garcia L 2015 Microstructure and mechanical properties of dissimilar friction stir welding of 6061-to-7050 aluminum alloys *Mater. Des.* **83** 60-5